

Contents lists available at [SciVerse ScienceDirect](http://www.sciencedirect.com)

Radiation Measurements

journal homepage: www.elsevier.com/locate/radmeas

Two-stage thermal stimulation of thermoluminescence

R. Chen^{a,*}, J.L. Lawless^b, V. Pagonis^c^a Raymond and Beverly Sackler School of Physics and Astronomy, Tel-Aviv University, Haim Levanon St., Tel-Aviv 69978, Israel^b Redwood Scientific Incorporated, Pacifica, CA 94044-4300, USA^c Physics Department, McDaniel College, Westminster, MD 21157, USA

ARTICLE INFO

Article history:

Received 21 September 2011

Received in revised form

20 December 2011

Accepted 10 January 2012

Keywords:

Thermoluminescence

Two-stage

Thermal stimulation

Simulation

Anomalous stability

ABSTRACT

A thermoluminescence (TL) model of two-stage stimulation of electrons into the conduction band is discussed. This release of the carriers is assumed to take place via an intermediate localized excited state. Electrons are thermally stimulated from the trap into an excited state and then thermally released into the conduction band from which they may either be retrapped or recombine with holes in centers. The model resembles the previous “semi localized” model, but we concentrate only on recombination of electrons that go through the conduction band. It also bears similarity to the effect of thermally-assisted optically stimulated luminescence (OSL) previously discussed in the literature.

The model is studied by solving the set of the relevant four simultaneous differential equations which govern the process during heating or isothermal decay. Using different sets of parameters, we can get pseudo-first-order, pseudo-second-order as well as intermediate cases, which are identified by their symmetry coefficient. Once the effective order is established, different analytical methods are used to determine the effective activation energy and frequency factor. We used the peak-shape methods, the various heating rate (VHR) method and the method based on the change of phosphorescence decay with temperature. The results are compared to the parameters used in the simulation. In many cases, the effective activation energy is equal to $E_1 + E_2$ where E_1 and E_2 are, respectively, the activation energies for the first and second stage of thermal stimulation. The numerical simulation results are accompanied by an analytical treatment using the usual quasi-steady assumption. Unusual cases, in which the effective frequency factor and the effective retrapping probability coefficient are temperature dependent, are identified. Some cases in which the effective activation energy is close to E_1 rather than $E_1 + E_2$ are identified and discussed. The relevance of this possible situation to the evaluation of the stability of TL signals is also considered, and a possible effect of anomalous stability is predicted.

© 2012 Elsevier Ltd. All rights reserved.

1. Introduction

A number of works have dealt with the semi localized transition (SLT) model of thermoluminescence (TL) (see: Mandowski, 2005, 2006; Pagonis, 2005; Kumar et al., 2007; Pagonis and Kulp, 2010). In this model, one electron trapping state, N , and one kind of recombination center, m , are considered. The trap is assumed to have an excited state, n_e . During the heating stage, electrons can be raised thermally from n to n_e . From the excited state, they can either recombine with a nearby hole in center, or retrap back to the ground state, or be thermally released into the conduction band. Once in the conduction band, the electron can retrap into the excited electron state or recombine with a hole in the center. Both the localized transition from the excited state into the

recombination center and the delocalized transition from the conduction band into the center are assumed to produce measurable TL. As pointed out by Pagonis (2005), the SLT model can explain the failure of the peak-shape methods to yield the correct activation energies.

In the present work, we concentrate on a somewhat more limited model. We keep the same energy levels, but assume that the TL results only from recombination of free electrons in the conduction band with holes in centers. No direct transition from the excited state into the recombination center is allowed. With this, more concise two-stage model, we study the relation between the parameters inserted into the model and the effective parameters determined by different analytical methods such as the peak-shape method or the various heating rate method. The relevance of this situation to the stability of the TL signal is considered.

One should note that this concept of two-stage stimulation of TL is close to that of the thermally-assisted optically stimulated luminescence (OSL). This effect of temperature dependent OSL has

* Corresponding author. Tel.: +972 3 6408426; fax: +972 9 9561213.
E-mail address: chenr@tau.ac.il (R. Chen).

been first described by Hütt et al. (1988) and later discussed by several authors (e.g. Spooner, 1994; McKeever et al., 1997; Chruścińska and Przegiętka, 2010). McKeever et al. (1997) discuss a number of models explaining the temperature dependent OSL which include the possibility that light excites the electron into an excited state, from which it may be thermally excited into the delocalized band with a thermally activated probability which follows an $\exp(-E/kT)$ law. The present model is rather similar, except that we assume both stages of the stimulation to be thermal.

2. The model

The two-stage energy-band model is shown in Fig. 1. The trapping state with concentration N (cm^{-3}) and instantaneous occupancy n (cm^{-3}) is shown, as well as the excited state n_e . The activation energy for this transition is E_1 (eV) and the frequency factor is s_1 (s^{-1}). Once the electron is in the excited state, it can either retrap with a probability of p (s^{-1}) or be thermally excited into the conduction band. The activation energy for this transition is E_2 (eV) and the frequency factor is s_2 (s^{-1}). The instantaneous concentration of electrons in the conduction band is denoted by n_c (cm^{-3}). From the conduction band, the electrons can be retrapped into the excited state with a retrapping probability coefficient of A_n ($\text{cm}^3 \text{s}^{-1}$), or recombine with a hole in the center with a probability coefficient of A_m ($\text{cm}^3 \text{s}^{-1}$). This recombination is assumed to produce the TL photons with an instantaneous intensity I . The emitted light is shown by the thick arrow. At the end of the initial excitation by irradiation, the number of trapped holes, m_0 , is equal to the total number of trapped electrons, namely, $n_0 + n_{e0}$, however, since the excitation is performed at a relatively low temperature, n_{e0} can be considered to be relatively small so that $n_0 \approx m_0$. The recombination of the electron from the conduction band with the hole in the center is assumed to produce the TL photon. In accordance with the detailed balance principle and neglecting electronic degeneracies, the values of the frequency factor for the first transition, s_1 , and the retrapping probability, p , must, according to Halperin and Braner (1960), to be equal: $s_1 = p$. Similarly, using the detailed balance principle, Mott and Gurney (1948) have shown that A_n and s_2 are connected by the equation

$$\frac{s_2}{A_n} = \frac{(2\pi m_e^* kT)^{3/2}}{h^3}, \quad (1)$$

where m_e^* is the effective mass of the electrons in the conduction band, k is Boltzmann's constant and h is the Planck constant. A typical value of the right-hand side is 10^{19}cm^{-3} . Thus, for example, if $s_2 = 10^{13} \text{s}^{-1}$, then $A_n \approx 10^{-6} \text{cm}^3 \text{s}^{-1}$.

The simultaneous differential equations governing the process during the heating stage, shown in Fig. 1 are

$$\frac{dn}{dt} = -s_1 n \exp(-E_1/kT) + p n_e, \quad (2)$$

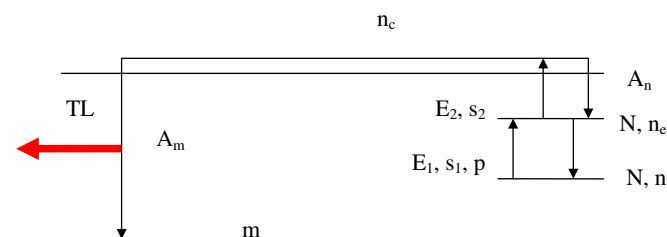


Fig. 1. Energy level diagram of the two-stage model.

$$\frac{dn_e}{dt} = A_n(N - n - n_e)n_c + s_1 n \exp(-E_1/kT) - s_2 n_e \exp(-E_2/kT) - p n_e, \quad (3)$$

$$I = -\frac{dm}{dt} = A_m m n_c, \quad (4)$$

$$\frac{dn_c}{dt} = \frac{dm}{dt} - \frac{dn}{dt} - \frac{dn_e}{dt} \quad (5)$$

Note that in writing the first term in Eq. (3) one assumes that no retrapping into the excited state n_e is possible if there is an electron either in the ground state of the trap or in its excited state.

3. Analytical considerations

Normally, excited states relax quite rapidly compared to the time scales of TL experiments. If so, using Eq. (3), we can employ the approximation

$$\frac{1}{n_e} \frac{dn_e}{dt} \ll [p + s_2 \exp(-E_2/kT)] \quad (6)$$

With typical values of p in the range of 10^6 – 10^9s^{-1} or higher, this is likely a very accurate assumption. Consequently, we can model the excited state as quasi-steady. Applying the condition (6) to Eq. (3), it then follows that

$$n_e = \frac{A_n(N - n - n_e)n_c + ns_1 \exp(-E_1/kT)}{p + s_2 \exp(-E_2/kT)} \quad (7)$$

Substituting this into the conservation equation for the ground state of trap n , Eq. (2), yields

$$\frac{dn}{dt} = p \frac{A_n(N - n)n_c + ns_1 \exp(-E_1/kT)}{p + s_2 \exp(-E_2/kT)} - s_1 \exp(-E_1/kT)n, \quad (8)$$

where, consistently with the quasi-steady assumption, we have assumed the excited state to have a small population, $n_e \ll (N - n)$. Rearranging Eq. (8) puts this formula into the following form,

$$\frac{dn}{dt} = -ns_{eff} \exp[-(E_1 + E_2)/kT] + A_{n,eff}(N - n)n_c, \quad (9)$$

where

$$s_{eff} = \frac{s_1 s_2}{p + s_2 \exp(-E_2/kT)}, \quad (10)$$

and

$$A_{n,eff} = \frac{p}{p + s_2 \exp(-E_2/kT)} A_n. \quad (11)$$

Equation (9) looks exactly like the conventional one-stage kinetics (see e.g. Eq. (5.1) in Halperin and Braner (1960)) except that the rate constants s_{eff} and $A_{n,eff}$ are temperature dependent and the effective activation energy is $E_1 + E_2$. There are two cases to consider with relation to Eqs. (10) and (11). If

$$s_2 \exp(-E_2/kT) \ll p, \quad (12)$$

then $s_{eff} = (s_1/p)s_2$ and $A_{n,eff} = A_n$. Eq. (9) reduces to

$$\frac{dn}{dt} = -ns_2 \exp[-(E_1 + E_2)/kT] + A_n(N - n)n_c, \quad (13)$$

exactly the original equation when thermal excitation is directly into the conduction band, but with $E_1 + E_2$ and s_2 .

On the other hand, if

$$s_2 \exp(-E_2/kT) \gg p, \quad (14)$$

then $s_{eff} = s_1 \exp(E_2/kT)$ and $A_{n,eff} = (p/s_2) \exp(E_2/kT) A_n$. The governing equation is now

$$\frac{dn}{dt} = -s_1 n \exp(-E_1/kT) + (pA_n/s_2) \exp(E_2/kT) (N - n) n_c. \quad (15)$$

The former case obviously corresponds to the usual circumstances where s_{eff} and $A_{n,eff}$ are constants. The latter case in which p is relatively small may yield strange behavior. The exponential temperature dependence of s_{eff} has the effect of reducing the effective energy from $E_1 + E_2$ to E_1 . Also, s_{eff} reduces here to s_1 . The exponential temperature dependence of $A_{n,eff}$ may also influence the shape of the TL peak. However, as long as Eq. (14) holds, the second term on the right of Eq. (15) is often small, which may reduce the equation to regular first-order, with the parameters E_1 and s_1 as seen in the numerical results above.

In the next section we present some results of numerical simulations that demonstrate some features of TL under the present model.

4. Numerical results and analysis

In this section, we present some results of simulations of specific physical situations within the double-stage excitation model, reached by solving numerically Eqs. (2)–(5) for appropriately chosen sets of trapping parameters. The numerical solution was performed using the MATLAB ode15s program. Fig. 2 depicts the results of a peak governed by Eqs. (2)–(5) with the parameters given in the caption. Note that since this is a one-trap one-center model, we can assume that at low temperature, when n_e and n_c are negligibly small, $n_0 = m_0$. The heating rate used was $\beta = 1 \text{ K s}^{-1}$ in curve (a) and 2 K s^{-1} in curve (b). The peak shown looks like a simple first-order peak, with a symmetry factor of $\mu = 0.44$. We can use the peak-shape method for evaluating the effective activation energy. The expression given by Chen (1969) is

$$E_{\omega 1} = kT_m \left(2.52 \frac{T_m}{\omega} - 2 \right). \quad (16)$$

Inserting from the simulated results, we get $E_{\omega 1} = 1.244 \text{ eV}$, rather close to the given value of $E_1 + E_2$. Inserting this value into the expression for the maximum of a first-order TL peak,

$$s = \frac{\beta E}{kT_m^2} \exp(E/kT_m), \quad (17)$$

we get from curve (a) $s_{eff} = 2.5 \times 10^{11} \text{ s}^{-1}$, closer to s_1 than to s_2 .

Let us consider the difference between curves (a) and (b). As expected, the peak shifted to a higher temperature at the higher heating rate. We used the equation for determining the activation energy using various heating rates (see e.g., Chen and Winer, 1970), namely

$$E = k \frac{T_1 T_2}{T_1 - T_2} \ln \left[\frac{\beta_1 \left(\frac{T_2}{T_1} \right)^2}{\beta_2 \left(\frac{T_1}{T_2} \right)^2} \right]. \quad (18)$$

The resulting activation energy from the simulated glow peaks here was 1.28 eV, again, very close to the given value of $E_1 + E_2$. Inserting this value into Eq. (17) yields $s_{eff} = 5.6 \times 10^{11} \text{ s}^{-1}$, again rather close to the inserted value of s_2 .

Fig. 3 shows the simulated decay of phosphorescence on a semi-log scale. Line (a) shows the decay at 450 K and line (b) at 460 K. Whereas the 450 K line is straight up to 500 s, the 460 K line deviates from linearity from $\sim 250 \text{ s}$ on. The reason is that the model we are dealing with is not simply of one-trap and one-center due to the transition through the excited state, and therefore, one cannot always expect a simple exponential decay. Let us analyze, however, these decay curves as if they were related to simple first-order kinetics. Assuming an exponential decay, the exponent α can be written as

$$\alpha = s_{eff} \exp(-E_{eff}/kT). \quad (19)$$

By writing this equation for two temperatures, T_1 and T_2 , one gets α_1 and α_2 respectively. Dividing one by the other, s_{eff} is eliminated, and one gets

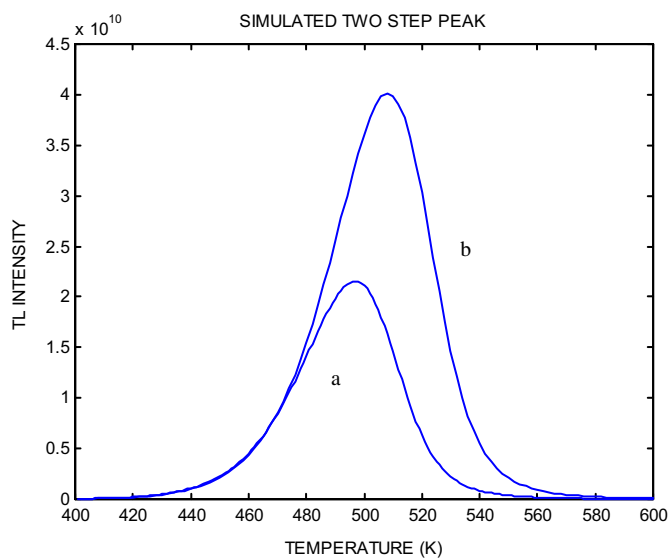


Fig. 2. Simulated results of a TL peak governed by the two-stage model, Eqs. (2)–(5). The parameters used were $E_1 = 0.8 \text{ eV}$; $E_2 = 0.5 \text{ eV}$; $p = s_1 = 10^{11} \text{ s}^{-1}$; $s_2 = 10^{12} \text{ s}^{-1}$; $A_n = 10^{-8} \text{ cm}^3 \text{ s}^{-1}$; $A_m = 10^{-6} \text{ cm}^3 \text{ s}^{-1}$; $N = 10^{13} \text{ cm}^{-3}$. The initial occupancies were $n_0 = m_0 = 10^{12} \text{ cm}^{-3}$. The heating rate was $\beta_1 = 1 \text{ K s}^{-1}$ in curve (a) and $\beta_2 = 2 \text{ K s}^{-1}$ in curve (b).

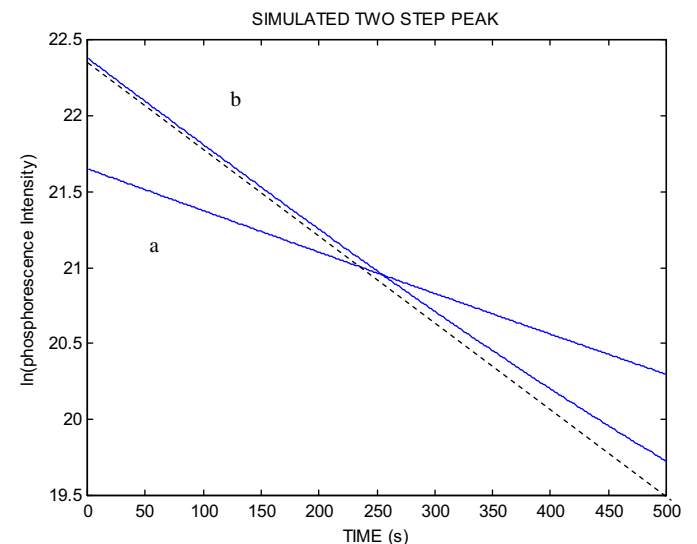


Fig. 3. Simulated decay of phosphorescence at (a) 450 K and (b) 460 K with the same set of parameters as in Fig. 2. The results are shown on a semi-log scale. The dashed line is a straight line added to show the slight deviation of line (b) from linearity on the semi-log scale.

$$E_{eff} = k \frac{T_1 T_2}{T_1 - T_2} \ln \frac{\alpha_1}{\alpha_2} \quad (20)$$

The two slopes are evaluated from Fig. 3 as $\alpha_1 = 5.56 \times 10^{-3}$ and $\alpha_2 = 2.6 \times 10^{-3}$. Inserting into Eq. (20), we get $E_{eff} = 1.36$ eV. Substituting into Eq. (19), we get $s_{eff} = 4.4 \times 10^{12} \text{ s}^{-1}$. These two values are rather close to $E_1 + E_2$ and s_2 , respectively.

With the same parameters, we checked the stability of the traps at room temperature (RT), 300 K (curve (a)) and at 310 K (curve (b)). The results of the simulations are shown in Fig. 4. In the simulation, the sample was “held” at 300 K or 310 K for 10^8 s, and the occupancy of the traps was monitored. After this period of more than 3 years, the concentrations of electrons and holes reduced by $\sim 1.3\%$ in curve (a) and by $\sim 6.5\%$ in curve (b). Using again Eq. (20), we get $E_{eff} = 1.31$ eV, and from Eq. (17) we get $s_{eff} = 1.32 \times 10^{12} \text{ s}^{-1}$, very close to $E_1 + E_2$ and s_2 , respectively.

Fig. 5 depicts the results of TL simulations with significantly smaller recombination probability coefficient, $A_m = 10^{-10} \text{ cm}^3 \text{ s}^{-1}$. As could be expected, the peak looks like a second-order peak. Curve (a) is with a heating rate $\beta_1 = 1 \text{ K s}^{-1}$ and curve (b) with $\beta_2 = 2 \text{ K s}^{-1}$. The shape factor is $\mu_g = 0.528$, like a typical second-order peak. The activation energy is determined by the second-order equation

$$E_{\omega 2} = kT_m \left(3.54 \frac{T_m}{\omega} - 2 \right) \quad (21)$$

The value reached here is $E_{\omega 2} = 1.26$ eV, in very good agreement with $E_1 + E_2$. Also, the various heating rates method, Eq. (18), yields here 1.32 eV, again with very good agreement with the sum of energies.

Let us turn now to the more interesting cases in which $s_2 \exp(-E_2/kT) \gg p$ (see Eq. (14)). Like in Fig. 2, we use a high recombination probability of $10^{-6} \text{ cm}^3 \text{ s}^{-1}$ and we change here $s_1 = p$ to be 10^6 s^{-1} . The results are shown in Fig. 6 for heating rates $\beta_1 = 1 \text{ K/s}$ in curve (a) and $\beta_2 = 2 \text{ K/s}$ in curve (b). The symmetry factor here is $\mu_g = 0.41$, typical of first-order peaks. By using the first-order peak-shape method, Eq. (16), we get here $E_{eff} = 0.82$ eV, very close to the inserted value of E_1 . Using the various heating rate

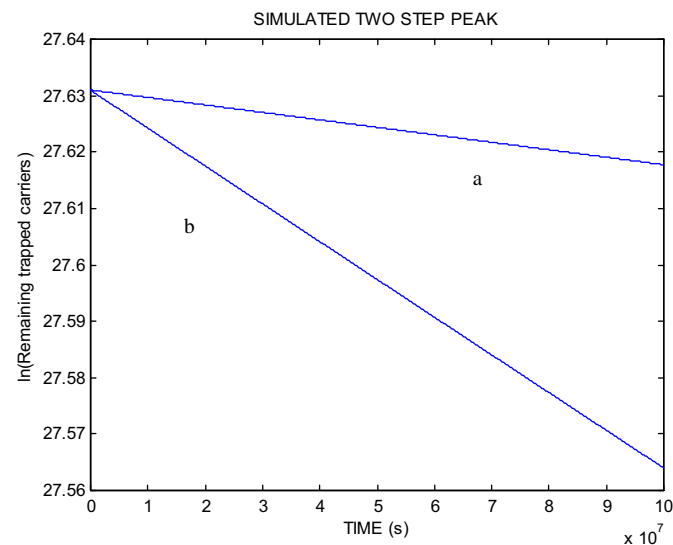


Fig. 4. Simulated results of the stability of the signal on a semi-log scale. With the same set of parameters, the remaining concentration of carriers in traps is shown for up to 10^8 s at (a) 300 K and (b) 310 K.

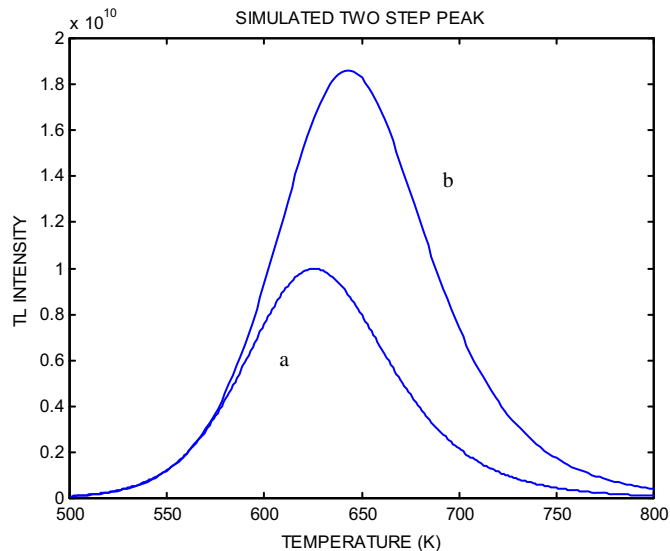


Fig. 5. Simulated results of a TL peak governed by the same model. The parameters used are the same as in Fig. 2 except that $A_m = 10^{-10} \text{ cm}^3 \text{ s}^{-1}$, 4 orders of magnitude smaller. The heating rate was $\beta_1 = 1 \text{ K s}^{-1}$ in curve (a) and $\beta_2 = 2 \text{ K s}^{-1}$ in curve (b).

equation, Eq. (20), we get $E_{eff} = 0.8$ eV. Both these values are associated in this case with E_1 . Using Eq. (17), we get $s_{eff} = 1.43 \times 10^6 \text{ s}^{-1}$, very close to the given value of s_1 .

With the same set of parameters, we simulated the decay of phosphorescence. This is shown in Fig. 7, for 490 K (a) and 500 K (b). From the slopes of the two lines, given on a semi-log scale, and using Eq. (20) we get $E_{eff} = 0.86$ eV, rather close to the inserted value of E_1 . Finally, for this set of parameters, we studied the stability around room temperature. Like in the case depicted in Fig. 4, we simulated the decay of the trapped carriers with time, up to 10^8 s at 300 K and 310 K with the same set of parameters. The results are practically the same as in Fig. 4, and thus the effective activation energy is here too $\sim 1.3 \text{ eV} = E_1 + E_2$, and $s_{eff} \sim s_2$.

It should be noted that in some intermediate cases we found effective activation energies between E_1 and $E_1 + E_2$ and effective frequency factors between s_1 and s_2 .

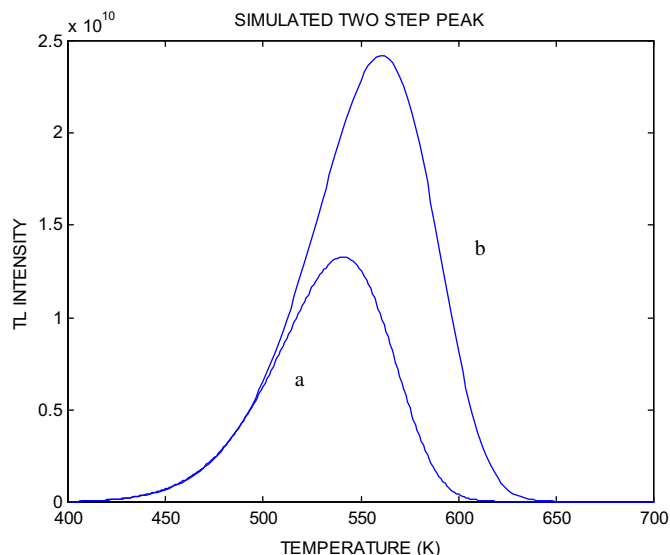


Fig. 6. Same as Fig. 5 but with $A_m = 10^{-6} \text{ cm}^3 \text{ s}^{-1}$ and $p = s_1 = 10^6 \text{ s}^{-1}$.

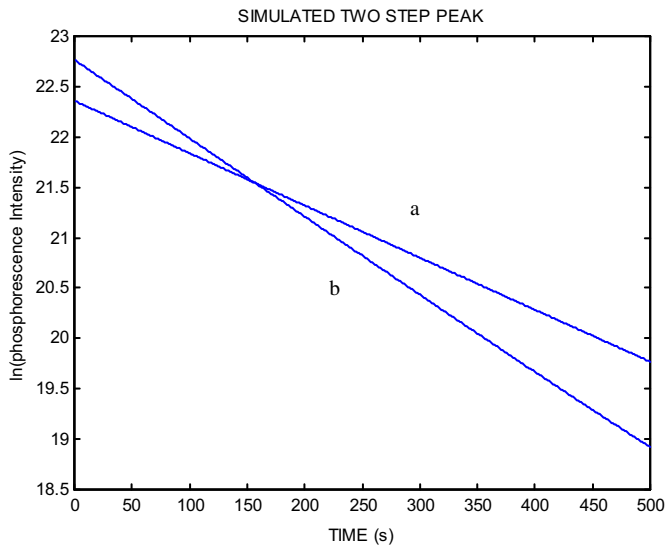


Fig. 7. The decay of phosphorescence with the same parameters as in Fig. 6, at (a) 490 K and (b) 500 K.

5. Discussion

In this work, we have studied the expected behavior of TL peaks associated with the two-stage thermal excitation shown in Fig. 1. By using analytical considerations as well as numerical simulation we demonstrated that first and second-order peaks can be reached for appropriate choices of the sets of relevant parameters. The effective values of the activation energy and the frequency factor as determined from the simulated results are compared to the inserted values of the parameters. Whereas in many cases the effective activation energy is found to be $E_1 + E_2$, cases where the value is close to E_1 are also recognized.

With the choice of $s_1 = p = 10^{11} \text{ s}^{-1}$, the condition (12) is fulfilled through the whole relevant range of temperatures. Here we always got $E_{\text{eff}} \approx E_1 + E_2$ and $s_{\text{eff}} \approx s_2$ as expected from the discussion next to Eq. (12) when $s_1 = p$ as, indeed, is assumed. This includes the results reached by the peak-shape method and the various heating rates method (Fig. 2), the phosphorescence decay at two temperatures (Fig. 3) and the stability of trapped carriers at two temperatures close to room temperature (Fig. 4). With the same choice of $s_1 = p = 10^{11} \text{ s}^{-1}$, but with small recombination, $A_m = 10^{-10} \text{ cm}^3 \text{ s}^{-1}$, we also get $E_{\text{eff}} \approx E_1 + E_2$ (Fig. 5). Here we have a second-order peak. Note that in the “original” second-order case, the intensity is given be (see Chen et al., 1983)

$$I = -\frac{dn}{dt} = \left(\frac{sA_m}{NA_n}\right) \exp\left(-\frac{E}{kT}\right) n^2. \quad (22)$$

The analogous equation in the present situation is

$$I = -\frac{dn}{dt} = \left(\frac{s_{\text{eff}}A_m}{NA_{n,\text{eff}}}\right) \exp\left(-\frac{E_1 + E_2}{kT}\right) n^2. \quad (23)$$

From Eqs. (10) and (11) it is obvious that the temperature dependent term cancels out and therefore, the term in the first parentheses is constant, $s_1 s_2 / p A_n$, and since we always assume that $p = s_1$, the constant in the parentheses is simply s_2 / A_n . The result is that in the second-order case, the activation energy will always appear to be $E_1 + E_2$.

In order to simulate TL, phosphorescence and stability in cases where the condition (14) holds, we have taken the same set of

parameters but with significantly smaller value of p , namely, $p = s_1 = 10^6 \text{ s}^{-1}$. Here, with the relatively low value of p , it is obvious that at the peak occurring $\sim 550 \text{ K}$ the effective activation energy is very close to E_1 , in accordance with the discussion concerning Eq. (13) above. The same value is reached from the slopes of the logarithm of the phosphorescence decays in Fig. 7. However, the two slopes of the room temperature stability simulation that, as stated above, look practically the same as in Fig. 4, yielding effective activation energy of $\sim E_1 + E_2$. This point may have implications concerning the suitability of a TL peak for dating. From the properties of the TL peak or phosphorescence decay at relatively high temperature, one may deduce the activation energy which is relatively low ($\sim E_1$). However, the room temperature stability is governed by a significantly higher energy ($\sim E_1 + E_2$). The expression for the effective lifetime is

$$\tau_{\text{eff}} = \left(1/s_{\text{eff}}\right) \exp\left(E_{\text{eff}}/kT\right). \quad (24)$$

From the above mentioned numerical results, the effective values of the parameters deduced from the TL peak are $E_{\text{eff}} = 0.8 \text{ eV}$ and $s_{\text{eff}} = 1.43 \times 10^6 \text{ s}^{-1}$. From this, one gets at room temperature (300 K) $\tau_{\text{eff}} = 1.9 \times 10^7 \text{ s}$, around 7 months. However, as pointed out above, the real stability is associated with $E_{\text{eff}} = 1.3 \text{ eV}$ and $s_{\text{eff}} = 10^{12} \text{ s}^{-1}$ which yields at 300 K $\tau_{\text{eff}} = 6.9 \times 10^9 \text{ s}$, about 220 years. One may thus expect a possible “anomalous stability”, an effect which is the opposite of the quite well known “anomalous fading”. With the parameters in hand, one may predict a relatively fast decay of a signal whereas the real decay may be significantly slower. Note that a similar effect has been discussed, under entirely different circumstances, by Wintle (1975). While discussing the thermal quenching of TL in quartz, Wintle states that it “causes the initial-rise method of trap depth determination to give spuriously low results which erroneously implies instability of a peak which is suitable for dating”. The simple model presented in this work may also account for this kind of effect.

References

- Chen, R., 1969. On the calculation of activation energies and frequency factors from glow curves. *J. Appl. Phys.* 40, 570–585.
- Chen, R., Winer, S.A.A., 1970. Effects of heating rates on glow curves. *J. Appl. Phys.* 13, 5227–5232.
- Chen, R., Huntley, D.J., Berger, G.W., 1983. Analysis of thermoluminescence data dominated by second-order kinetics. *Phys. Stat. Sol.* (a) 79, 251–261.
- Chruścińska, A., Przegiętka, K.R., 2010. The influence of electron-phonon interaction on the OSL decay curve shape. *Radiat. Meas.* 45, 317–319.
- Halperin, A., Braner, A.A., 1960. Evaluation of thermal activation energies from glow curves. *Physiol. Rev.* 117, 408–415.
- Hütt, G., Jaek, I., Tchonka, J., 1988. Optical dating: K-feldspars optical response stimulation spectra. *Quarter. Sci. Rev.* 7, 381–385.
- Kumar, M., Kher, R.K., Bhatt, B.C., Sunta, C.M., 2007. A comparative study of the models dealing with localized and semi-localized transitions in thermally stimulated luminescence. *J. Phys. D. Appl. Phys.*, 5865–5872.
- Mandowski, A., 2005. Semi-localized transitions model for thermoluminescence. *J. Phys. D. Appl. Phys.* 38, 17–21.
- Mandowski, A., 2006. Topology-dependent thermoluminescence kinetics. *Radiat. Prot. Dosimetry.* 119, 23–28.
- McKeever, S.W.S., Bøtter-Jensen, L., Agersap Larsen, N., Duller, G.A.T., 1997. Temperature dependence of OSL curves: experimental and theoretical aspects. *Radiat. Meas.* 27, 161–170.
- Mott, N.F., Gurney, M.A., 1948. *Electronic Processes in Ionic Crystals*, p. 108. Dover, N.Y.
- Pagonis, V., 2005. Evaluation of activation energies in the semi-localized transition model of thermoluminescence. *J. Phys. D* 38, 2179–2186.
- Pagonis, V., Kulp, C., 2010. Simulations of isothermal processes in the semilocalized transition (SLT) model of thermoluminescence (TL). *J. Phys. D* 43, 175403 (8 pp.).
- Spooner, N.A., 1994. The optical dating signal from quartz. *Radiat. Meas.* 23, 593–600.
- Wintle, A.G., 1975. Thermal quenching of thermoluminescence in quartz. *Geophys. J.R. Astr. Soc.* 41, 107–113.